

# Submersible holocamera for microparticle investigation: problems and solutions

V.V. Dyomin, I.G. Polovtsev, A.V. Makarov, V.A. Mazur,  
A.A. Tarasenko,<sup>1</sup> N.N. Kovbasyuk,<sup>1</sup> and N.G. Mel'nik<sup>2</sup>

*Tomsk State University*

<sup>1</sup> *Scientific Research and Design Institute "Okeanografika," Gelendzhik*

<sup>2</sup> *Limnological Institute,*

*Siberian Branch of the Russian Academy of Sciences, Irkutsk*

Received July 3, 2003

Methods of pulsed holography have some advantages that are principally unachievable by other methods. Therefore, these methods can be efficiently used to study biological and medical particles, particles suspended in liquid, plankton, etc. This paper presents tentative results on development of a submersible holocamera for particle investigation. The camera employs an off-axis scheme with image transfer and a basic (transmitted) object beam. The characteristics of the optical scheme of particle image transfer are calculated numerically. A computer program is developed for modeling of the holography system with allowance for the photomaterial parameters. Laboratory breadboarding of the hologram recording system has been made. The results of calculations and laboratory experiments allow us to estimate the resolution of the holographic scheme as 100 micrometers with the recorded volume at the depth of 250 mm and 200 micrometers at the depth up to 500 mm.

## Introduction

Many problems in biology, medicine, ocean optics, and other fields of science and technology assume investigation of objects (in particular, biological objects) in a liquid medium. Such problems are, for instance, observation of the state of plankton, suspended particles in the surface sea layer at ecological monitoring of the sea/shore, study of the structure and dynamics of a cloud of suspended particles in the water depth in order to evaluate the effect of mining operations on ocean ecosystems, etc.

The methods of pulsed holography are most acceptable for studying movable particles in liquid media, because they have some advantages that are principally unachievable for other methods. They are:

recording of a 3D image of extended objects;

no effect on the object under study;

no need in the *a priori* data on the object under study;

possibility of recording, storage, and following laboratory decoding of the information about the object under study.

Accurate recording of such information as object size, shape, position per one hologram for the short time of a laser pulse ( $\tau_p$  ranges from 10 to 100 ns), as well as velocity in the case of double holograms permits the investigation of dynamic volume ensembles of objects. The recorded volume may be up to several thousands  $\text{cm}^3$ . The resolution of modern holographic methods (up to 10  $\mu\text{m}$ ) allows classification of objects and determination of their position and orientation. Therefore, the use of these methods is most expedient to study biological and medical particles, plankton,

and structure and dynamics of a cloud of suspended particles.

To apply holographic methods to such studies, one needs to have a proper submersible camera for hologram recording. The works on the use of holography for plankton recording were started in the 1970s. Thus, for example, Carder<sup>1</sup> studied the shape and size of depositing particles using their holographic images. Katz et al. in 1984 and O'Hern et al. (1988) developed the first underwater holographic system employing a pulsed ruby laser and applied it to measure the number and size of particles and bubbles in water at Catalina Island.<sup>2,3</sup> Characteristics of holographic methods at recording of microparticles in liquids are studied in Refs. 4–7, where the results on the use of hologrammetry for plankton studies in water reservoirs are presented.

Nowadays from the literature we know two submersible apparatuses (SA) used for underwater holographic recording of particles (see, for example, Refs. 2, 3, 8, 9). In Russia such instrumentation is lacking, mostly due to the absence of research programs on its development and difficulties in fabrication of specialized laser systems. In this paper we present tentative data on development of a submersible holographic camera: a chosen optical scheme and results of calculation and laboratory studies of its characteristics (largely, the resolution and scene depth).

When studying volume ensembles of particles in the reconstructed holographic image of a medium volume, it is necessary to find, identify, and study images of individual particles, which is a rather complicated and laborious process. Besides, holographic images of particles in a liquid have some

features absent in the case of recording in air.<sup>10–12</sup> One of them is appearance of aberrations because recorded objects are in a medium with one refractive index (water), while a hologram at the stage of its recording and reconstructed holographic images are in a medium with another refractive index (air). The ways to take these distortions into accounts are discussed in this paper.

## 1. Main features of holographic recording of objects in a liquid

### 1.1. Basic holographic schemes

Three basic schemes used for recording of volume ensembles of particles, namely, in-line scheme, off-axis scheme, and off-axis scheme with image transfer are illustrated in Fig. 1.

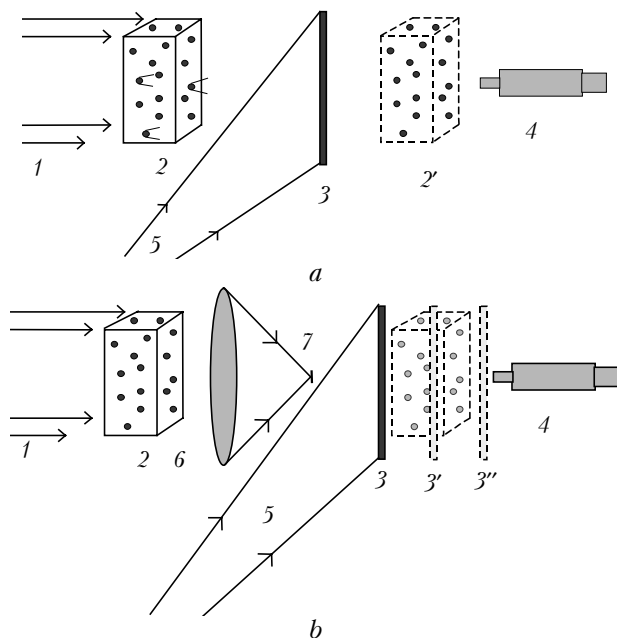


**Fig. 1.** Basic schemes of hologram recording: off-axis scheme (or in-line one without the reference beam 5) (a) and off-axis scheme with image transfer (b): illuminating beam 1, studied volume 2, its image at the stage of reconstruction 2'; photoplate (at the stage of recording) or hologram (at the stage of recording) 3; possible positions of a photoplate 3', 3''; magnifying optical system to study the holographic image 4; reference beam (at the stage of recording) or reconstructing beam (at the stage of reconstruction) 5; optical system for image transfer 6; mask 7.

In the in-line optical arrangement (Fig. 1a without reference beam 5) the object wave is formed by radiation scattered at recorded particles, while the reference one is formed by radiation passed without the interaction with particles. The in-line scheme is simple, but significantly limited in the particle concentration.

The off-axis arrangement (Fig. 1a) allows recording of ensembles with the far higher concentration of particles, since it employs a separate

reference beam 5 that does not path through the studied volume 2. Nevertheless, transparency of the medium, the object under study is, imposes objective restrictions on holography. For maximum efficiency of holographic imaging, that is, the possibility of determining geometric parameters of every individual particle in the volume, its transparency should be no lower than 80%. At the lower transparency of the medium, it is difficult to separate holographic images of particles against the background of speckles, and therefore the information about the particle size, shape, etc. is lost. Figure 1a shows also that after recording and photochemical processing the hologram 3 is illuminated by the reconstructing beam identical to the reference beam 5, and the reconstructed 3D holographic image 2' is studied using the magnifying optical system 4, for example, a microscope.

The resolution and the depth of the recorded object (scene depth) are mostly determined by the resolution and the homogeneous range of photomaterials used for hologram recording. It was found experimentally that holographic methods permit recording of particles with the minimum size of 2–3  $\mu\text{m}$ . However, such holographic images can be used only to detect a particle and determine its position in space, rather that to study its shape. Geometric parameters can be studied only for particles larger than 50  $\mu\text{m}$ , and the resolution becomes worse with the distance from a particle.

The off-axis scheme with image transfer is shown in Fig. 1b. In this case, we record the hologram of not the object 2, but its image constructed by the optical system 6 on a photomaterial; 3, 3', and 3'' are possible position of a photoplate at the stage of recording, the most widely used of them is position 3''. This scheme provides for the maximum distance to recorded objects. Besides, placing the mask 7 at the focus of image transfer optical system 6, we can realize the dark field method and thus increase the contrast of holographic images of particles. It should be noted that in this scheme the resolution is mostly determined by the optical system 6.

Note also that all the above schemes can be realized in transmitted light, while the reflected light can be used only in the off-axis optical arrangement and in the arrangement with image transfer.

Underwater holographic cameras described in some papers use classical in-line and off-axis arrangements. In Ref. 8, for example, both of these approaches are used simultaneously, and the off-axis layout uses side illumination of the recorded volume, practically, in the reflected light. This gives the maximum viewing angle for the recorded particles and thus provides for their reliable identification, which is especially important in plankton studies. At the same time, such a combination of the schemes required high laser pulse energy – 650 mJ (Nd:YAG laser with frequency doubling, wavelength of 532 nm, pulse duration less than 10 ns) and resulted in large size (1 m in diameter, 2.4 m in length) and mass (2.3 t) of the submersible apparatus.<sup>8</sup>

Besides, in most applications of underwater holography, the information obtained using such optical arrangements seems to be excessive. That is why we have chosen the off-axis scheme with the image transfer, illumination of the recorded volume in transmitted light, and filtering in the object beam (see Fig. 1*b*). Prior estimates showed that the use of a Nd:YAG laser with the pulse energy of 30–40 mJ is sufficient for recording holograms of objects in a liquid.

## 1.2. Preliminary holographic imaging

Figure 2 shows examples of the holographic images of particles in a liquid that illustrate the capabilities of holographic methods. These pictures largely correspond to small (up to several millimeters) objects with details about 50  $\mu\text{m}$  at different distances.

Objects were placed in an aquarium with fresh water, which provided for the maximum path length up to 1 m. The off-axis optical arrangement and the off-axis layout with image transfer were used. The object beam was realized by the basic scheme (transmitted

light). In different experiments, He–Ne, ruby, and Nd:YAG lasers were used as sources of radiation.

The results of the experiments suggest the possibility of holographing objects with details of about 50  $\mu\text{m}$  in water at the distance up to 0.5 m from the recording plane. At lower requirements to resolved details, the distance to an object can be increased. In the latter case, the restriction is determined by the power of the laser used. The Nd:YAG laser with frequency doubling is obviously useful, because its radiation (532 nm) is absorbed by water much weaker than, for example, the radiation of the ruby laser (694 nm).

It should be noted that many biological objects are transparent (semitransparent) or have such properties. As a rule, these fragments have focusing properties (for example, Figs. 2*e–j*). In Refs. 12 and 13 this property was used to determine the particle refractive index from a holographic image. The experimental error was equal to 10% and mostly connected with the accuracy of determination of the focal point position.

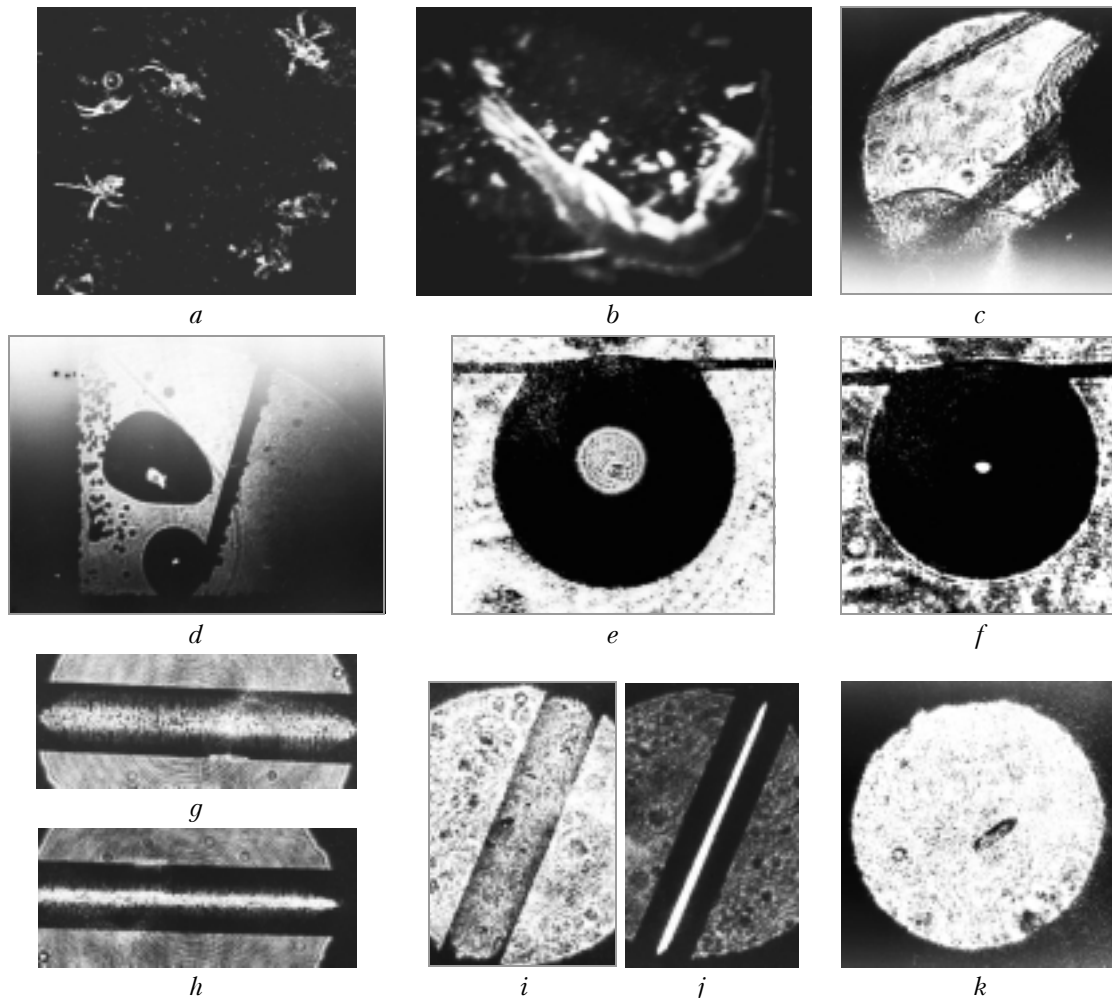


**Fig. 2.** Examples of holographic images of particles: Baikal plankton (size of 100–200  $\mu\text{m}$ ) (*a*); semitransparent fragment of macrohctopus body found in a holographic image (*c*); air bubbles (1–2 mm) floating in water (*d*); water droplet (*e*, *f*) in air at acutance at different planes of the holographic image: the central cross section of the droplet (*e*) and the focal point (*f*); cylindrical object (light guide) in air (*g*, *h*) at acutance at the central cross section (*g*) and the focusing line (*h*); the same but in water (*i*, *j*); infusorium in liquid (*k*).

### 1.3. Difference in refractive indices

One of the methodical problems in underwater holography recording of particles is removing aberrations in the reconstructed image. Aberrations arise, because objects are in water, while holograms are recorded and reconstructed in air. For the in-line optical arrangement, these aberrations are insignificant, because the reference and object beams are normal to the recording plane. In the off-axis layout (at illumination in the reflected light) the difference in the refractive indices leads to considerable aberrations. The most significant of them is astigmatism, which increases with the increasing object viewing angle in the reconstructed image. Image worsening can be minimized by reconstructing the hologram in air with the use of the radiation with the effective wavelength (that is, wavelength equal to the recording wavelength divided by the water refractive index).<sup>10</sup> For example, if objects in water are recorded holographically with the wavelength of 694 nm, the hologram in air should be reconstructed by the radiation with the wavelength of 521 nm (in practice, reconstruction with the use of argon laser radiation (514 nm) gives good results).<sup>10</sup>

When a hologram is recorded using the radiation of the Nd:YAG laser with frequency doubling (532 nm), it can be successfully reconstructed by the radiation of the He–Cd laser (442 nm).<sup>8</sup>

In Ref. 12 it was proposed to consider such distortions as recording a hologram of not the particle itself, but its image in the optical system “water–glass (window)–air” (illumination by the transmitted light is considered). It was shown that the position of the particle image can be corrected numerically, if the refractive indices of the media (water, glass, air) are known and interface positions are determined from the 3D holographic image. Such a numerical correction gives good results with the error no greater than 10%.

It should be noted that in the case of the off-axis arrangement with the basic (transmitted) object beam, the angles, at which the object beam is incident onto the photoplate at hologram recording, are close to zero, which allows us to expect minimum distortions that can be corrected numerically.<sup>12</sup>

## 2. Functional layout of submersible holocamera

From the preliminary experiments, estimates, and analysis of the literature, it follows that the off-axis optical arrangement with the basic (transmitted) object beam and filtering of low spatial frequencies (see Fig. 1) is most suitable for a submersible holocamera. The known cameras<sup>8</sup> ensure operation down to the depth of 100 m. We are developing an apparatus for studying depositing (in particular, near-bottom) particles at the depth down to 6000 m in the places of prospective mining. The camera is being developed with allowance for the design solutions of the Research & Design Institute “Okeangeofizika” and orientated at using standard optical elements.

The functional block-diagram of the optical part of the camera is shown in Fig. 3.

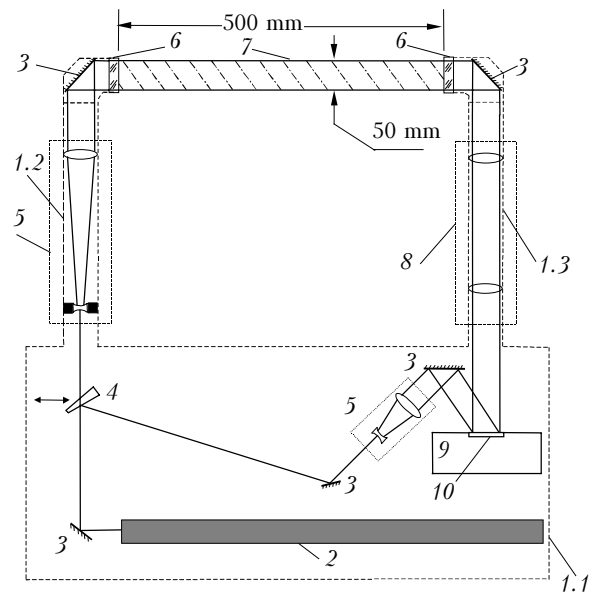


**Fig. 3.** Functional layout of the optical part of the system for underwater holographic recording: body 1 (platform 1.1 and remote rods 1.2 and 1.3); pulsed laser 2; mirrors 3; beam splitter 4; beam formers 5; windows 6; medium volume recorded 7; optical system for image transfer 8; shutter with photoplate holder 9; holographic photoplate 10.

It is assumed that a part of the optical components are assembled on the common platform 1.1, while another part is on two remote rods 1.2 and 1.3. The platform and rods are arranged perpendicularly.

The beam splitter 4 divides the radiation from the laser 2 into the reference and object beams. For realization of the in-line or off-axis optical arrangement, the beam splitter can be set on and off the beam axis.

The beam former 5 provides for the parallel beam 50 mm in diameter. The studied volume 7 is a cylinder 50 mm in diameter and 500 mm in length. The volume 7 is spaced by about 700 mm from the main SA body to minimize turbulent distortion of the studied volume by the SA body.

The optical system 8 transfers the images of the objects (plankton particles, solid suspended particles) being in the studied volume into the area of hologram recording 10.

It is obvious that the resolution and the scene depth here are mostly determined by characteristics of the optical system 8 (Fig. 3). Let us formulate the main requirements to the optical system 8.

The magnification factor within the recorded volume (500 mm) should not vary by more than 10%. This is needed for minimum longitudinal distortions at image transfer to the hologram recording plane. At the same time, it is necessary for the image to be transferred with demagnification, since at the stage of reconstruction the entire volume is scanned by planes with a magnifying optical system (for example, microscope). Therefore, the longitudinal dimensions

of the reconstructed holographic image of the studied volume should not be large.

The images of cross sections of the studied volume should be concentrated on one side from the recording medium. This requirement is also connected with the use of the magnifying optical system (for example, microscope) at the stage of reconstruction and ensures that any cross section of the reconstructed images is accessible for measurements.

The clear aperture of the illuminating beam was set equal to 50 mm.

The resolution should provide for observation of an object with the size as small as 100  $\mu\text{m}$ .

This optical system was calculated using the Prizma CAD system. As a result, the main parameters of the optical scheme for image transfer<sup>14</sup> were determined (summarized in the Table) and the corresponding objectives were selected.

The scheme 8 (see Fig. 3) is the Kepler telescopic system with the magnification of  $0.83^{\times}$  that consists of objectives with the focal lengths  $f_1 = 234$  and  $f_2 = 195$  mm.

This system (as can be seen from the Table) provides for the needed resolution for objects located on the axis and the resolution of about 150  $\mu\text{m}$  for objects located at an edge of the cross section of the studied volume.

### 3. Numerical simulation of holographing of particles in a liquid

To take into account the features of holographic recording of objects under various conditions, as well as characteristics of various photomaterials, we have developed a program for computer simulation.

The algorithm for simulation of the process of hologram recording involves three stages. At the first stage a particle is simulated. Its surface is synthesized by the known cross sections or specified analytically. At the second stage, using the tracing method, the particle is replaced by an equivalent amplitude-phase screen in its central cross section. At the third stage, having known the field distribution in the plane of the amplitude-phase screen, the field distribution in different planes of the holographing optical arrangement, such as the interface plane between media (if any) and planes at which lenses and photomaterial are located, is calculated using the diffraction integral. A plane reference wave incident at the given angle to the hologram axis was imposed onto the field distribution in the hologram recording plane. Using the intensity distribution in the resulting interference

pattern and taking into account the specified parameters of the photomaterial, we can calculate the amplitude transmittance of the hologram.

The process of reconstruction of the holographic image is simulated similarly. The hologram here is considered as an amplitude screen, while the field and intensity distributions in the given plane of the holographic image of an object are calculated using the diffraction integral. Figures 4 and 5 show the main interface windows of the program.



Fig. 4. Interface window of the program. Input of system parameters.

In this paper, we present the results of testing the program simulating the third stage. The processes of hologram recording and reconstruction were simulated for plane particles of arbitrary shape and size (larger than 100  $\mu\text{m}$ ) and the off-axis optical arrangement with image transfer. The holographing scheme is close to the design of the submersible holocamera under development. The length of the recorded volume was 500 mm, the diameter of the illuminating beam was 50 mm, and the illuminator thickness was 50 mm.

The image transfer system consisted of two objectives with the focal lengths  $f_1 = 234$  and  $f_2 = 195$  mm. The quality of the reconstructed holographic image was analyzed by the degree of image shape likeness to the initial object and the degree of edge smear.

Distance from object to illuminator of optical system, mm	Distance from last surface of optical system to image, mm	System magnification	Size of spot in the plane of best set, mm, object on the axis	Size of spot in the plane of best set, mm, object 25 mm off the axis
-5	51.59	-0.8125	0.050	0.050
-250	-69.50	-0.8125	0.055	0.110
-500	-193.20	-0.8125	0.061	0.150

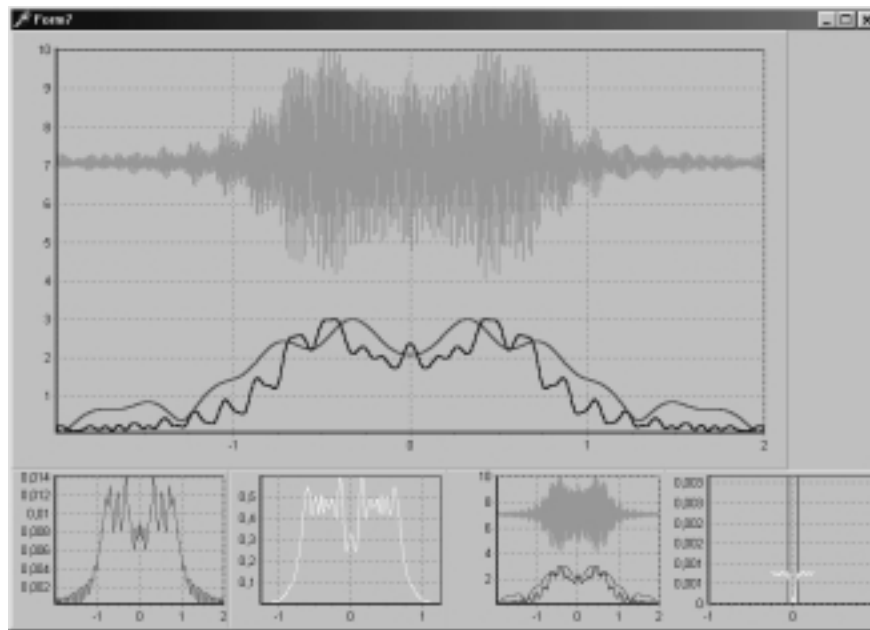


Fig. 5. Interface window of the program. Visualization of 1D scans of the intensity distribution.

Figures 6a–c shows the calculated intensity distributions in different planes of the holographing scheme and reconstruction of the holographic image of a triangle particle with the circumcircle radius of 500 μm located at the distance of 250 mm from the illuminator: initial image (a), water/illuminator interface (b), and reconstructed image (c).

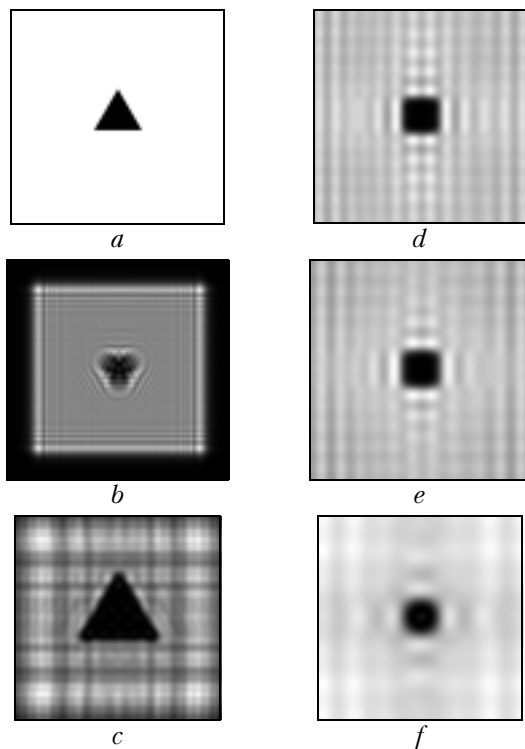


Fig. 6. Examples of calculated intensity distributions in different planes of the scheme of hologram recording and reconstruction.

Figures 6d–f show examples of reconstructed image in the case of simulating holograms of a square particle with a side of 100 μm at different distances from the illuminator: 50 (d), 100 (e), and 500 mm (f); the images are not reduced to the same scale. Particles of other regular shapes (rectangle, hexagon, circle, etc.) were considered as well. As the distance from an object to the plane of hologram recording increased, we observed the regular deterioration of the image.

The results of numerical simulation suggest the resolution to be about 100 μm for the holographing optical arrangement considered.

### 4. Results of laboratory breadboarding

The schematic layout of the laboratory mock-up is depicted in Fig. 7, and its photo is shown in Fig. 8. It employs the off-axis scheme with image transfer and the basic (transmitted) object beam. The radiation

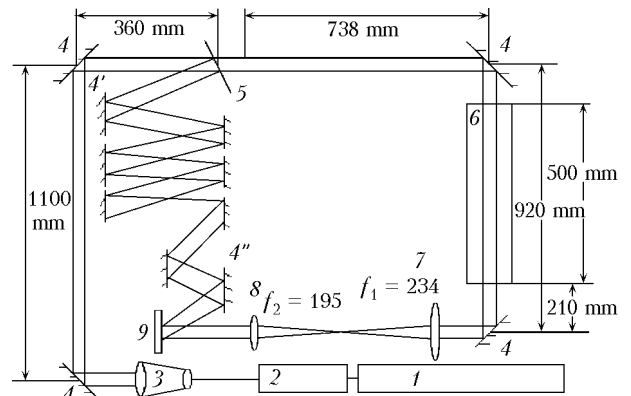


Fig. 7. Laboratory mock-up: pulsed laser 1; frequency doubler 2; beam former 3; mirrors 4; beam splitter 5; cell (recorded medium volume) 6; optical system for image transfer 7 and 8; photoplate 9.

source is a pulsed Nd:YAG laser with frequency doubling, wavelength of  $0.53\ \mu\text{m}$ , pulse duration of 30 ns, and pulse energy of 40 mJ.

The recorded volume was modeled by a cell with water, which housed model objects. The cell length was 500 mm, which corresponded to the planned length of a volume recorded by a submersible holographic camera. The diameter of the laser beam illuminating the volume was 50 mm. Thus, for one exposure the camera recorded the volume of about  $1000\ \text{cm}^3$ .

The image transfer system consisted of two objectives with the focal lengths of 234 and 195 mm, according to the previous calculations. In the laboratory mock-up, as in the anticipated submersible camera, the path of the object beam was about 2500 mm long.

The path-length difference of the object and reference beams is compensated for by a multiple-mirror delay line  $4'-4''$  in the reference beam. The arrangement of mirrors, collimators, and optical elements was maximum close to the design of the submersible camera. Thus, for example, the delay line  $4'-4''$  was constructed in such a way that it modeled a photoplate holder.

The intensity ratio of the object and reference beams was regulated by neutral density filters. To improve the contrast of holographic images of particles, we applied the dark field method by placing an opaque mask in the common focus of the objectives of the image transfer system.

In the experiments, this mock-up was used to record a series of holograms of model objects having various shapes with the size of  $100\ \mu\text{m}$  that were placed on a glass substrate. Holograms were recorded with the empty cell and the cell filled with water. To determine the scene depth, the recording plane was separated by different distances from the cell window: 50, 250, 380, and 480 mm.

The holographic images were reconstructed on a different laboratory mock-up. A He-Ne laser was used as a source of the reconstructing radiation.

The reconstructed holographic images of objects were observed visually with a microscope. Besides, using a digital camera with a specially made microattachment (with the magnification  $3\times$  and  $8\times$ ), the reconstructed images were entered into a PC and stored in the digital format.

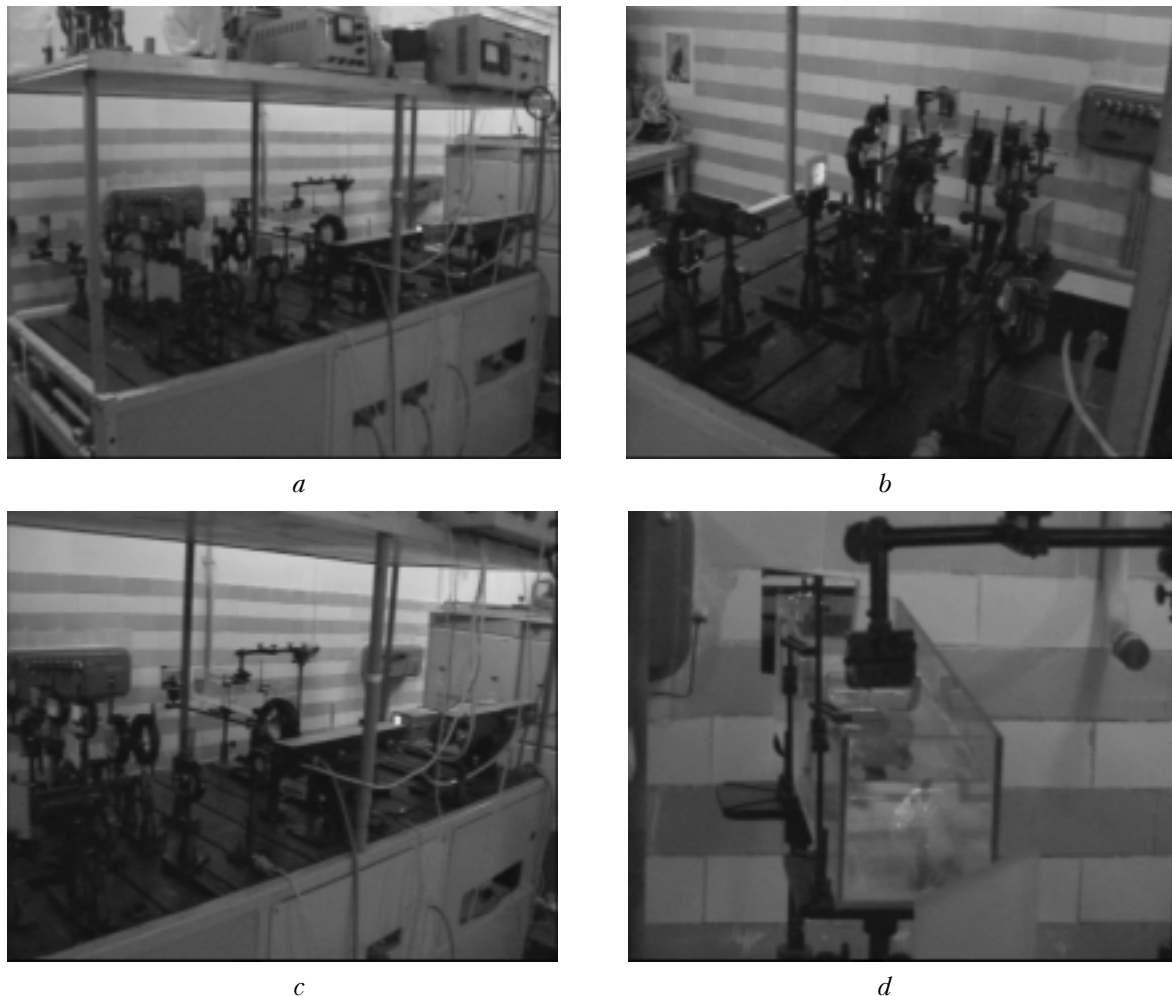
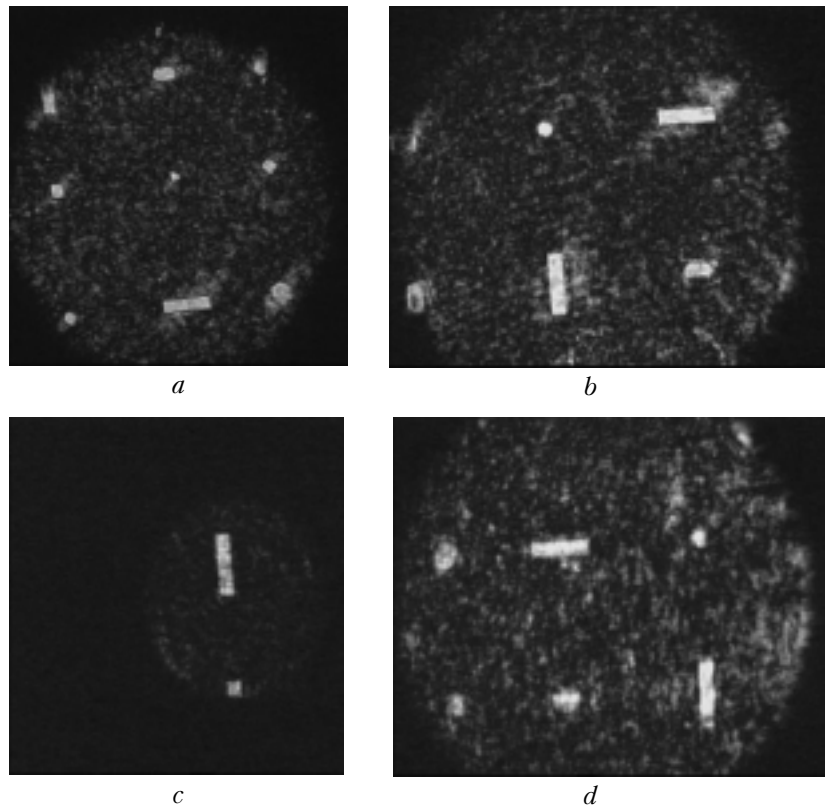


Fig. 8. General view of the laboratory mock-up (a); fragments of the mock-up (b, c); a cell with model objects under study (d).



**Fig. 9.** Photographs of real images of 100- $\mu\text{m}$  objects in water and air at different distances from the cell window: microobjective with  $3\times$  magnification (*a*, *b*, *d*); microobjective with  $8\times$  magnification (*c*); air, 50 mm from the cell window (*a*, *b*); water, distance from the cell window of 50 (*c*) and 250 mm (*d*).

Figure 9 depicts the photographs of real images of 100- $\mu\text{m}$  objects in water and in air at different distances from the cell window (the images in Fig. 9 are not reduced to the same scale).

Figures 9*a* and *b* illustrate objects spaced by 50 mm from the output window of the cell in air at  $3\times$  magnification. The mask for the dark field method had the size of 0.2 mm. Figure 9*c* depicts the objects spaced by the same distance, but in water at  $8\times$  magnification. The mask had the size of 0.08 mm.

With the increase of the scene depth, the sharpness and contrast of reconstructed images dropped down. Figure 9*d* depicts the images of the same objects in water at  $3\times$  magnification but spaced by 250 mm from the cell window.

With the further increase of the scene depth up to 380 and 480 mm from the cell window, the resolution decreased and the quality of obtained images of 100- $\mu\text{m}$  objects deteriorated.

## References

1. K.L. Carder and D.J. Meyers, *Opt. Eng.* **19**, No. 5, 734–738 (1980).
2. J. Katz, P.L. Donaghay, J. Zhang, S. King, and K. Russell, *Deep-Sea Research* **1** (46), Part I, 1455–1481 (1999).
3. E. Malkiel, O. Alquaddoomi, and J. Katz, *Meas. Sci. and Technol.* **10**, 1142–1152 (1999).
4. J. Watson, P.W. Britton, and A.C.S. Cran, *Opt. and Laser Technol.* **19**, No. 2, 97–101 (1987).
5. J. Watson, *Opt. and Lasers Eng.* **16**, 375–390 (1992).
6. E. Foster and J. Watson, *Opt. and Laser Technol.* **29**, No. 1, 17–23 (1997).
7. P.R. Hobson, E.P. Krantz, R.S. Lampitt, A. Rogerson, and J. Watson, *Opt. and Laser Technol.* **29**, No. 1, 25–33 (1997).
8. J. Watson, S. Alexander, G. Graig, D.C. Hendry, P.R. Hobson, R.S. Lampitt, J.M. Marteau, H. Nareid, M.A. Player, K. Saw, and K. Tipping, *Meas. Sci. and Technol.* **12**, L9–L15 (2001).
9. P.R. Hobson and J. Watson, *J. Opt. A: Pure and Appl. Opt.* **4**, S34–S49 (2002).
10. J.M. Kilpatrick and J. Watson, *Meas. Sci. and Technol.* **5**, 716–725 (1994).
11. V.V. Dyomin, *Proc. SPIE* **4678**, 382–392 (2001).
12. V.V. Dyomin and S.G. Stepanov, *Atmos. Oceanic Opt.* **11**, No. 7, 577–581 (1998).
13. V.V. Dyomin, "Holographic method for determination of the refractive index of particles in disperse media," Patent No. 2124194. Russia, G01N21/45. No. 94043766; Application from Dec. 13, 1994; Registered in the State Registry of Invents of the RF on Dec. 27, 1998.
14. G.V. Simonova, V.V. Dyomin, and I.G. Polovtsev, in: *Proceedings of 7th Int. Sci. Tech. Conference on Optical Methods for Flow Studies* (Moscow, 2003), pp. 280–283.